

Dr. 2615

LA-8777-PR

Progress Report

MASTER

R4169

①

333
5/8/81 T.S.

Superconducting Magnetic Energy Storage

(SMES) Program

January 1—December 31, 1980

University of California



LOS ALAMOS SCIENTIFIC LABORATORY

Post Office Box 1663 Los Alamos, New Mexico 87545

DISTRIBUTION OF THIS DOCUMENT IS UNLIMITED

SUPERCONDUCTING MAGNETIC ENERGY STORAGE (SMES) PROGRAM

January 1—December 31, 1980

Compiled by

John D. Rogers

ABSTRACT

Work is reported on the development of two superconducting magnetic energy storage (SMES) units. One is a 30-MJ unit for use by the Bonneville Power Administration (BPA) to stabilize power oscillations on their Pacific AC Intertie, and the second is a 1- to 10-GWh unit for use as a diurnal load leveling device. Emphasis has been on the stabilizing system. The manufacturing phase of the 30-MJ superconducting coil was initiated and the coil fabrication has advanced rapidly. The two converter power transformers were manufactured, successfully factory tested, and shipped. One transformer reached the Tacoma Substation in good condition; the other was dropped enroute and has been returned to the factory for rebuilding. Insulation of the 30-MJ coil has been examined for high voltage effects apt to be caused by transients such as inductive voltage spikes from the protective dump circuit. The stabilizing system converter and protective energy dump system were completed, factory tested, and delivered.

All of the 5-kA superconducting cable has been made. Specifications for a nonconducting dewar were developed and an RFQ was issued for manufacturing quotations. Bid responses are being evaluated. The seismic support system to hold the 30-MJ coil in the dewar has been designed. The 5-kA helium vapor-cooled lead design is nearly complete. The 4.5 K refrigerator was completed, installed in the trailer, and successfully factory tested in the trailer configuration. The cold box was damaged in shipping and the entire unit was returned to the factory for repair. The trailer-mounted heat rejection system was completed, tested, and delivered. The design for the trailer-

mounted gas recovery system was completed and an order placed to build the unit. Most of the hardware for the control and data acquisition system has been obtained. The control logic is in an advanced state of development and software is being prepared. An Interface Working Agreement among BPA, the Los Alamos National Laboratory, DOE Albuquerque Office, and the Division of Energy Storage Systems was completed to define the BPA's and the Los Alamos National Laboratory's project responsibilities. An analytical study was performed for a simple wire-rope-supported superconducting cable for a 1- to 10-GWh diurnal load leveling SMES unit.

The superconductor application VAR (SAVAR) control program studied the use of small superconducting coils for economic application to electric utility systems.

I. SUMMARY

The goal of the Los Alamos National Laboratory's SMES program is to develop electrical units to store energy in a magnetic field around a coil or inductor. The magnetic field is created by an electric current flowing in a conductor that is in a superconducting state. Many materials, such as niobium-titanium, lose their resistance to electric currents, that is, become superconducting at low temperatures. Electrical utilities can use 1 to 10 GWh SMES units to meet diurnal variations in consumer power demand. During the night, when consumption is low, generators can supply energy to the unit. During the day, when demand is high, energy can be drawn from the SMES unit. In another application, smaller 30 MJ (8.3 kWh) SMES units can be used to damp out the short term power oscillations that in complex electrical grids, sometimes limit maximum power transmission.

This report describes the progress made in the design and hardware development of the 30 MJ stabilizing SMES unit and testing of superconducting cable for the unit. The components that must be considered for both systems are the superconductor itself; the coil; the dewar, which will contain the coil and liquid helium to cool it to a superconducting state; the cryogenic equipment to make liquid helium and keep it cold; the electrical equipment to connect the coil to the power grid; and, finally, the monitor and control equipment to control the charge and discharge of the coil.

The 30 MJ superconducting coil design by General Atomic Company (GA) was completed, a design review held, and coil manufacture started. The 5 kA superconducting cable development and stability testing was successfully completed. All the cable for the coil was manufactured by New England Electric Wire (NEEW) and delivered to GA for coil winding. About half the pancake coils were wound. Because the stabilizing unit is connected to a public utility system, careful design of the coil mounting in the nonconducting dewar

has been undertaken to cope with Zone C seismic effects. This part of the design is now complete.

The design of the 5 kA helium vapor cooled leads which penetrate the dewar lid to carry the current to the 30 MJ coil is nearly complete. The 4.5 K refrigerator, which will be used to supply liquid helium to the 30 MJ superconducting coil dewar and compensate for the several heat leaks, was factory installed by the manufacturer, the CTI Division of Helix Corporation, in a van type trailer supplied by the Los Alamos National Laboratory and successfully tested. Damage incurred to the cold box during shipment requires factory repair and the unit was returned to CTI.

The closed loop heat rejection system with cooling tower, which will serve as the waste heat dump for the refrigerator and gas recovery compressors, was completed and delivered after factory testing.

The trailer mounted, gas recovery unit was designed and placed on order. The unit will serve to pump vaporized helium gas to a railroad tank car for storage.

A nonconducting dewar is to be used with the 30 MJ coil to avoid magnetic coupling with the dewar wall to keep energy losses low. Specifications for the dewar were written, an RFQ issued, and bid responses are being evaluated.

The converter, which will interface between the BPA Pacific AC Intertie at the Tacoma Substation and the 30 MJ superconducting coil, was completed by the Robicon Corporation, and factory tested under both high current and high voltage conditions. The converter was shipped to the Los Alamos National Laboratory and has had all controls and interlocks checked.

The power transformers between the intertie and the converter were made by Niagara Transformer Company. These were factory tested to specification and shipped to the BPA Tacoma Substation. One arrived without incident and the other was dropped from a truck in Indiana. It was badly damaged and returned to the factory for rebuilding.

Transient electrical effects, possibly from the operation of the protective dump resistor system, were examined analytically to determine the necessary insulation withstand voltage for the coil, vapor cooled leads, and other components.

The stabilizing unit is to be operated by microwave link from Portland, OR to the unmanned Tacoma, WA substation. Most of the control hardware and data acquisition equipment for the system was purchased. Control logic is nearly all developed and software is being written.

Meetings were held with BPA staff to establish site requirements and to identify work assignments for BPA and the Los Alamos National Laboratory for installation of the stabilizing unit at the BPA Tacoma Substation. An interface Working Agreement among BPA, the Los Alamos National Laboratory, and DOE was completed. The document defines BPA's and the Los Alamos National Laboratory's responsibilities. The site plan for the Tacoma Substation SMES installation was developed by joint agreement between BPA and the Los Alamos National Laboratory. An artist's concept of the arrangement of equipment is

shown in Fig. 1. The converter with the power transformers on either side with the HVAC feeder bus is shown to the left rear. The seismically supported nonconducting annular dewar and 30 MJ superconducting coil are in the center foreground, and the refrigerator and gas handling and heat rejection units are to the right. Not shown in the figure is the railroad tank car for gas storage.

Previously designed superconducting cables for 1 to 10 GWh diurnal load leveling SMES units have been unusually complicated and not readily adapted to field fabrication. An analytical study was performed for a simple wire rope supported superconducting cable for a large SMES unit.

The Superconductor Application VAR (SAVAR) control program has studied the use of small superconducting coils for economic application to electric utility systems. The early analysis of the economic study is that a superconducting VAR control system might save 15% over 30 years and requires development of a very high technology system. The concept has been demonstrated by experiments conducted with both normal conducting and superconducting coils as circuit components.

II. BONNEVILLE POWER ADMINISTRATION STABILIZING SMES UNIT

A. Introduction

The Pacific Northwest and southern California are part of the Western US Power System and are connected by two 500 kV, ac power transmission lines, collectively referred to as the Pacific AC Intertie, and one +400 kV dc transmission line, the Pacific HVDC Intertie. The two ac lines have a thermal rating of 3500 MW, and the dc line has a rating of 1440 MW.

The stability of the Western Power System is affected by relative weakness of the tie provided by the 905 mile long Pacific AC Intertie. In fact, studies made before energization of the Pacific AC Intertie showed that negatively damped oscillations with a frequency of about 20 cpm were likely to occur. In 1974 negatively damped oscillations with a frequency of 21 cpm (0.35 Hz) were observed. The peak to peak oscillation on the Pacific AC Intertie was about 300 MW. Subsequent to these instabilities, the BPA installed equipment on the HVDC intertie to use as a power source to modulate the power flow in the HVAC intertie as a means of damping the oscillations. The maximum possible power modulation is +40 MW. The modulation has increased the stability limit of the Pacific AC Intertie from about 2100 MW to 2500 MW whenever the HVDC Intertie is operating. However, the HVDC Intertie does not operate continuously. The line availability is 89.5%, and the southern terminal was down for six months at one time as a result of earthquake damage. A back-up stabilizing system could be used. Late in 1975, representatives of BPA and Los Alamos developed the concept of installing a small SMES unit for the purpose of providing system damping similar to that now available by modulation of the intertie.

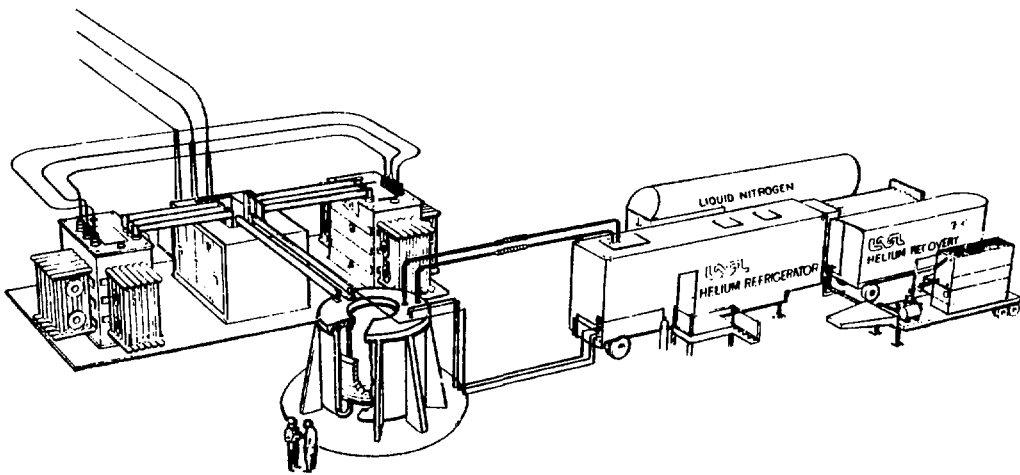


Fig. 1. 30 MJ SMES stabilizer system layout for BPA Tacoma Substation.

B. Superconducting Coil Design and Manufacture (Henke, Rogers, Schermer; General Atomic Co. staff)

On January 13 and 14, 1980, a panel of six outside experts in superconducting magnet technology met at GA with representatives of GA and Los Alamos for the final design review on the 30 MJ coil. The panel felt that the coil design had no serious deficiencies. Several items were identified that deserved additional consideration. Under structural engineering, the panel suggested a number of buckling or deformation modes, all of which were analyzed and found to be no problem. Objections to the vertical tie bolts led to the present system of 1 in. diam bolts preloaded with Belleville washers. Under electrical engineering, several suggestions were accepted, which produced longer breakdown paths for electrical creep and mechanically sturdier insulation. Other suggestions, related to noncritical items, were accepted at the discretion of GA.

GA has contracts, on the basis of competitive bidding, to procure all necessary materials and fabrication services for the coil construction. All material with long lead times, such as G-10 CR, were purchased. All parts directly needed for winding of the coils with the 5 kA cable are either now at GA or are arriving on a schedule such that they will not delay coil manufacture. Ten double pancake coils were completed by mid December, and the cable for the remaining 10 double pancakes was completed by NEEW and has been shipped to GA.

Each double pancake is wound on an inner support ring, or bobbin, fabricated by wet layups of epoxy, reinforced with a combination of glass fabric and glass roving. The epoxy is a mix of Epon 828 and V-40 hardener, cured at room temperature. Initial tests were run on sample lengths of material; and, after difficulties were encountered, a full bobbin was sacrificed to provide

further test material. The specific problem noted was that the support rings developed cracks upon thermal cycling to 77 K. The cracks did not propagate through the glass fabric layers. They were found to develop extensively upon sudden cooling but also, to a lesser extent, upon a cooling cycle roughly characteristic of that to be used in operation. An additional oven cure of the material did not improve the situation.

The main function of the support rings during operation is to retain the shear pins that transfer seismic shear loads vertically through the coil. In a shear test, a cracked sample performed to the limit of the shear pin without failing. Further, warm and cold bending tests in both transverse directions showed no detectable difference in either stiffness or ultimate strength between cracked and uncracked samples. Therefore, the rings should perform acceptably in service although they will exhibit some cracking during cooling.

C. Superconducting Cable (Harkleroad, Henke, Prince, Smith, Schermer, Yarnell)

The goals of the conductor development activity for 1980 were to test the prototype version of the final conductor completely and to write detailed fabrication instructions and specifications to permit GA to purchase the 5 kA cable. The adopted design is shown in Fig. 2. The cable specifications are given in Table I. This cable has passed all planned mechanical and electrical tests and meets or exceeds all requirements.

The testing program was an extension of that developed in 1979 and reported in the immediately previous annual progress report. Mechanical tests investigated the static and fatigue properties of the cable under transverse compressive loading. Electrical tests were performed to investigate conductor stability as well as for quality assurance on both superconductor and the copper stabilizer wires.

1. Superconductor. A total of 2.2×10^6 ft of superconducting strand was finally received, tested, and accepted as meeting specifications. The 340,000 ft of conductor purchased in 1979 had an average measured critical current 30% above the minimum acceptable value, or 50% above the actual operating requirement.

2. Copper. Although there are six copper wires cabled around each superconducting strand to make first subcables, compaction reduces the copper requirement by 15%. Accordingly, 11.5×10^6 ft (14,000 lbs) of soft, No. 24 AWG (0.511 mm) PDOF copper wire were purchased from Phelps Dodge Corp. After annealing for 2 hrs at 325°C, the wires had an RRR, the ratio of electrical resistance at 300 K to resistance at 4.0 K, of 321 ± 25 . An acceptance value of 180 had been set for this ratio. The chance of fabricating a first level cable with RRR < 180 from six randomly selected copper wires, is small.

The copper was shipped directly to the cable fabricator, NEEW, and was packaged on spools that fit directly on the NEEW cabler to eliminate respooling.

3. Conductor Cleaning. Much of the superconducting strand had been on hand for 18 months and showed surface oxidation. Some of the surface contamination, probably from inadequate removal of drawing lubricant before final

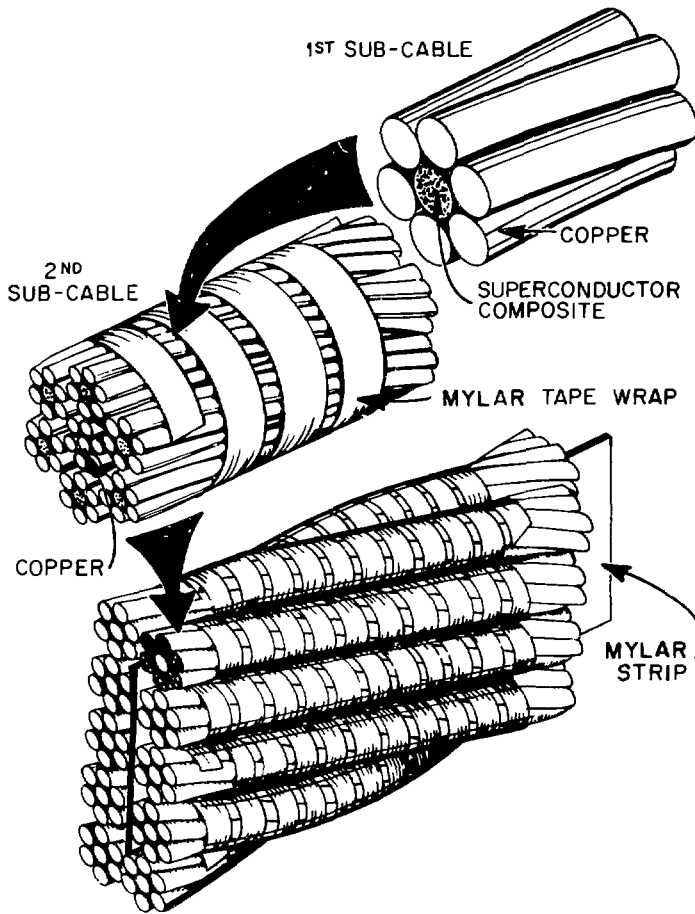


Fig. 2. 5 kA, low loss cryostable superconducting cable.

annealing, was worse than most. Auger spectroscopy revealed carbon and oxygen penetration of 1×10^{-8} m into the surface. As a precaution, an electrolytic cleaning operation was specified prior to cabling. An improvement in cleanliness was made by not using lubricant to compact first level cable. The indication from stability experiments is that improved surface cleanliness will aid thermal and electrical contact among first subcable wires.

4. First and Second Subcables. Cabling and compaction increases the electrical resistivity of the copper enough to require annealing after the first subcable is formed. One QA sample was drawn from each annealing lot and given an RRR test at Los Alamos. All 26 samples were tested, yielding an RRR of 324 ± 32 in excellent agreement with the original material. The entire 2.2×10^6 ft of first subcable were formed with one diamond compaction die that, although unlubricated, showed no detectable wear. Experimental second sub-cables had been formed on a low speed, planetary cabling machine. The development of making the second subcable on a high speed tubular cabling machine with no significant decrease in RRR, resulted in a schedule reduction of several months and a large cost reduction.

TABLE I
CABLE SPECIFICATIONS FOR 30 MJ COIL

A. Superconductor Composite Core	
Area of NbTi, mm ²	4.85 x 10 ⁻²
Filament diameter μ m	6.5
Number of filaments	1464
Strand diameter, mm	0.511
Cu to NbTi ratio	2.94:1
Twist pitch, mm, and direction	5.0; R.H.
B. First Subcable: Six copper wires cabled about one core	
Uncompacted diameter, mm	1.52
Compacted diameter, mm	1.37
Overall Cu to NbTi ratio	26.7:1
Twist pitch, mm, and direction	13.5; L.H.
C. Second Subcable: Six first subcables around a stranded, insulated copper core	
Diameter, mm	4.11
Twist pitch, mm, and direction	34.9; R.H.
Insulation type	Mylar,* adhesive
Insulation size, mm	0.15 x 6.4
Insulation pitch, mm, and direction	8.64; L.H.
D. Finished Cable: Ten second subcables around a Mylar strip	
Strip dimension, mm	15 x 0.25
Conductor dimension, mm	23.6 x 7.6
Twist pitch, mm, and direction	200; L.H.

*duPont trademark.

5. Cable Insulation. Preliminary stability experiments had indicated that relatively small gaps in an insulating wrap on a cable were very effective in permitting heat transfer to the liquid helium. Mylar strip, 0.25 in. wide and 0.005 in. thick, perforated with two staggered rows of 1/16 in. holes on 1/8 in. centers, appeared to provide sufficient ventilation while simultaneously preventing accidental contact between second subcables. Several experiments were done with such insulation. The use of perforated strip did not overcome the additional expense of perforation and the fabrication problems produced by the lack of adhesive on the strip. Therefore, the final conductor employs unperforated, adhesive backed, 0.005 in. thick by 0.25 in. wide Mylar tape wrapped with 0.040 in. gaps. Loss calculations show that a short between second subcables can be tolerated at an approximate rate of one short per one hundred conductor twist pitches or about one short every 60 ft. Resistance measurements performed after the conductor was wound into final coils by GA show that any pair of second subcables shows one or two shorts per 1500 ft. Further, the resistance across the short is 10 m Ω , considerably larger than that assumed in the calculation. The result is that the intercable

shorts are expected to have no noticeable effect on ac losses or on current sharing.

6. 5 kA Production Cable. After numerous trials, the conductor dimensions given in Table I were chosen to give a well compacted cable with little or no mechanical damage to the subcables and the insulation. Once this last parameter was determined, in mid September, NEEW proceeded with full production. One half the final 5 kA cable has been received by GA, and the remainder has been shipped.

7. Testing of Cable. Electrical and mechanical tests of the 5 kA cable were concluded successfully. Stability measurements were conducted to determine recovery to the superconducting state after having gone to the normal conducting state. Joints between second subcables simulating those in the 30 MJ coil were tested. Both axial and radial loading tests were performed to simulate possible wear effects from cyclic Lorentz forces.

An experimental program in which the stability of second level cable samples was investigated as a function of heat transfer geometry, magnetic field, and insulation type was conducted over a period of several years. The program concluded this year with the selection of 0.005 in thick Mylar tape as the conductor insulation.

In a final test, a 7 m length of preproduction, 5 kA conductor, with the second subcables soldered together at the ends to form a bifilar sample, was wound in a single layer on a G-10 mandrel, fitted with support teeth and insulating strips to match the actual heat transfer environment in the 30 MJ coil. A single second subcable or all 10 subcables could be heated simultaneously. When a single second subcable was heated, no normal zones were observed in neighboring strands until, at a current rather larger than the recovery current for the heated strand, the zones were able to propagate through the solder joints between the second subcables. Thus, not only does the possibility exist to drive a single strand normal in a cabled conductor but for it to remain normal without affecting the other subcables. The recovery heat flux for the single subcable case was about 15% larger than that for the case with all subcables heated. The finished conductor is expected to carry up to 8.2 kA at 2.8 T and recover, if only one second subcable goes normal, and 7.9 kA at 2.8 T, if all the second subcables go normal. These currents are well into the current sharing region for the superconductor and considerably above the 4.9 kA operating current of the 30 MJ coil.

In the 30 MJ coil, an interpancake joint set consists of 10 individual joints between separated pairs of second subcables. Resistance measurements were taken on two prototype interpancake joint sets prepared by GA. In the first set, 9 of the joints had a resistance between 20 and 25 n Ω , at 1 or 2 T, whereas the tenth had 75 n Ω . Several of the joints, including the anomalous one, were peeled apart for examination. There were no obvious differences among the joints or flaws in any of them. GA then prepared the second set in which the second subcables were strongly pressed together and in which a better fluxing/tinning technique was used. All 10 of the second set of joints had resistance between 12 and 20 n Ω at 1 T.

A simple resistance calculation, which has considerable experimental backing, indicates that the joints should have resistance of 1 to 2 n Ω between

rectangular monolithic conductors. An average resistance of 20 Ω per joint produces a total Joule heating of 1 W in the 30 MJ coil, which is acceptable. Further, the higher resistance decreases ac losses in the joint structure and actually decreases the sum of the Joule heating plus ac losses.

Each second subcable in the 30 MJ coil has its own pair of power leads, which place an equal resistance of approximately 100 $\mu\Omega$ in series with each cable. This resistance will override the variation in resistance among cables due to joint variations or cold welds in the superconductor and should assure equal sharing of the 4.5 kA average current.

Axial load in the 30 MJ coil is supported by the interturn stainless steel strap and transmitted from layer to layer through 1/4 in. thick G-10 plates, perforated and grooved for cooling. Calculations by GA indicated sufficient margin against fatigue failure for this design, even in the case where one web between perforations has failed for some reason. The actual stresses generated when the narrow edge of the steel strap bears on the G-10 plate are difficult to model analytically, and a fatigue experiment was devised to verify the calculations.

The test used a model vertical section through the coil, five layers high by five turns wide by 4 3/4 in. long and included one plate with a "failed web." Compressive load was applied normal to the G-10 plates. The specimen was subjected to 1.1×10^7 stress cycles at 300 K at 116% of the expected maximum load in the 30 MJ coil and an additional 750,000 cycles at 4 K at 130% of maximum load. All testing was done by the Fracture and Deformation Division of NBS, Boulder, CO under contract to Los Alamos.

Stress-strain data showed no change in sample compliance during the experiment. Further, the compliance value was in approximate agreement with that used by GA in its calculations and is not a critical number in any case. Finally, an inspection of the test model revealed virtually no visible wear. The steel straps imbedded slightly in the G-10 plates, but the grooves were considerably less than 0.001 in. deep and create no problem. A small amount of glass dust was knocked loose from rough machined G-10 surfaces, so that GA has been asked to sand lightly and bead blast all such surfaces.

Mechanically, the weakest part of the conductor is the Mylar insulation. To control ac losses, it is important that shorts not develop between second level cables during the coil lifetime. The only significant cyclic load applied to the conductor is radial compression, that is, pressure normal to the wide face. Calculations show that the most highly stressed region is in the thirteenth turn at the axial midplane, with the stress depending on the transverse modulus of elasticity of the conductor. Calculated values range from 200 psi if $E = 1.3 \times 10^4$ psi to 420 psi if $E = 2 \times 10^5$ psi. The measured conductor modulus depends to a large extent on mechanical history, because there is a certain amount of "lost motion" in the as-fabricated material. The fatigue tests were performed before as-built modulus measurements became available. Preliminary measurements indicated a value of $E = 2 \times 10^4$ psi, so that a test based on $E = 2 \times 10^5$ psi was thought to be very conservative. Cyclic loading at 4 K can be conducted at a rate of ~500,000 cycles per day. A larger load at 10^6 cycles was used to simulate the effect

of 10^8 cycles. A study of existing data between 10^5 and 10^6 cycles for steel, copper, cloth based phenolic, and glass based epoxy indicates that a stress multiplier of 1.5 should conservatively cover the worst case. Therefore, the test was conducted between a maximum stress of $1.5 \times 420 = 630$ psi and a minimum stress of $2/3$ this value. Tests were performed by NBS Boulder with much of the same equipment as used for the axial fatigue test.

The sample was a full scale coil section, two turns high in the axial direction, four turns thick in the radial direction, and 4 in. long. Preproduction conductor was used. Electrical leads, attached to all of the second level cables in seven out of eight conductors, were continuously monitored for intercable shorts as the sample underwent 1.1×10^6 stress cycles while immersed in liquid helium. No shorts developed in this process and no damage was observed when the sample was disassembled.

The conductor as wound onto the 30 MJ pancake is compressed radially by a force of 600 lbs applied by a phenolic roller bearing on the overlying steel strap. This roller compacts the cable and removes most of the lost motion without damaging the conductor. As the radial build increases, the degree of compaction becomes less because each turn rests on the elastic foundation of the preceding turns. The measured modulus of the compacted coil is 270,000 psi after 3 turns and 100,000 after 23 turns. A uniform modulus of 270,000 psi has been used in a stress code by GA to check whether the coil will perform as desired when energized, that is, that all turns will remain in compression. The largest calculated radial stress is 450 psi, which is not significantly beyond the value assumed in designing the fatigue test.

D. Nonconducting Dewar (Schermer, Thullen, Weldon; Bennett, Butler, Ferdinand, Q-13)

Dewar design could not proceed until the seismic support design was determined. Consequently, procurement was delayed until the dewar has become the critical path item for the project.

Because the coil cycles continuously at a frequency of 0.35 Hz, the inner liquid helium vessel must be made of glass reinforced epoxy to avoid eddy current heating which would occur in a metal walled dewar. The outer room temperature vessel can be constructed either of a suitable plastic or of 300 series stainless steel. The lid can be constructed either of glass reinforced epoxy, fabric reinforced phenolic, or 300 series stainless steel. Further, the vessels can be assembled with either demountable or permanent seals. RFQs have been issued covering various combinations of these options for the vessels and bid responses are being evaluated. The lid, which is the complex interface between the coil electric and support systems, cryogenic system, and vacuum system, is still under detailed design. Lid fabrication is not expected to be a critical path procurement item.

1. Mechanical Design. Conceptually, the dewar is a nested set of open mouthed, toroidal shells. Figure 3 shows a version in which the vacuum space is sealed by a permanent closure between the outer room temperature and inner liquid helium vessels. This option avoids possible difficulties with O-ring seals on epoxy glass surfaces, but makes repairs within the vacuum space more difficult. Continuous vacuum pumping will be provided for the vacuum space to handle helium diffusion through the inner vessel.

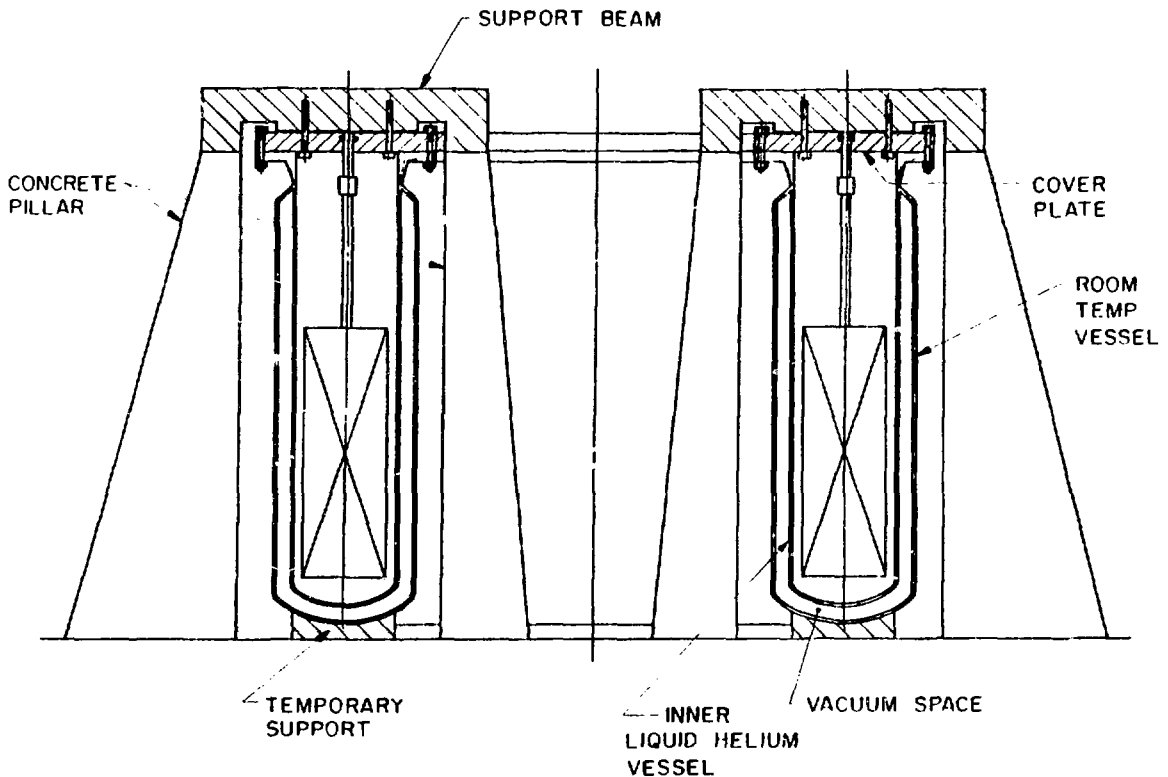


Fig. 3. Cross section through conceptual design of dewar and external support system.

The vessels are subject to normal working pressure loads, encountered during operation, which are essentially constant, that is, not cyclic. In addition, there are specified fault pressure loadings that should, in practice, never be encountered because these pressures are above the release pressures for safety vents and rupture discs. For normal working pressures the vessel is required not to fail catastrophically under the specified load, nor fail by creep, nor by fatigue if the working loads are applied 1,000 times. For fault pressures, the vessel or cover plate must not fail catastrophically, for instance by buckling, and the O-ring seals must not leak. Under all conditions, the material of the vessel is required to remain leak tight as determined by soap bubble or helium leak detector tests, as appropriate. The normal working pressure for the liquid helium vessel is 15 to 30 psia, and for the vacuum space, the normal pressure is 0 psia with external ambient pressure of 15 psia. The fault pressure for the liquid helium vessel is 50 psia, and for the vacuum space, the fault pressure is 20 psia, again with 15 psia external ambient pressure.

For a metal vessel and metal cover plate, there are additional magnetic loads, due to eddy currents, that are smaller than the pressure loads. A metal vessel also produces nonuniform potential gradients in the coil under transient conditions. For these reasons, a metal vessel would be a distinct second choice except that a metal vessel represents a far more highly developed technology than a plastic vessel and should cost less. A metal lid is favored because of the complexity of the penetrations and the need to transmit seismic loads through the lid material.

Numerical design studies have been conducted on the glass reinforced liquid helium vessel and on the flange region between the lid and helium vessel in Fig. 3.

A number of preliminary structural design studies were performed on various portions of the vessel. The design parameters were based on allowable stresses, σ_A , as follows:

For stainless steel $\sigma_A < 2/3 \sigma \text{ yield} = 20 \text{ ksi};$

For G-10 $\sigma_A < 5 \text{ ksi}$ for long term loading,
a creep limitation;

$\sigma_A < 40\% \sigma \text{ ultimate}$ for short term; or
transients = 16 ksi.

Where seal integrity is important, deformation limits were considered. Loading conditions can be referred to the schematic cross section of Fig. 4. This figure gives notations of various parameters and loadings used in these studies. The internal design pressure, p , is taken to be 30 psia during normal operation and 50 psia during coil quench. G-10 is assumed to have isotropic material properties of Young's modulus = 2×10^6 psi and Poisson's ratio = 0.3.

Two dewar lids were considered. For a 300 series stainless steel lid with a working stress of 20 ksi, the maximum stress is the governing criteria, and a lid of 1 1/4 in. nominal thickness, t_{lid} , is required. The penetrations must be reinforced in accordance with the stress concentrations they produce. Rules governing the type and placement of the reinforcing such as in the ASME Boiler and Pressure Vessel Code¹ can be used to ensure an adequate design.

If a G-10 lid is used, the governing criteria is the contribution of the slope of the lid to the opening of a proposed O-ring seal at the flanges. If this opening is restricted to 0.020 in., a 2.5 in. thick lid is required. The maximum bending stress for simple supports at fault conditions will be about 2 ksi.

The flanges and seals between the lid and helium dewar were examined. The two options for the flange design considered were the bolted through double flange, a flange for both the inner helium vessel and outer room temperature vacuum vessel as depicted in Fig. 4, and the bolted through single flanged helium vessel with a skirt for attaching the vacuum vessel as depicted in Fig. 3. Flange and lid rotation under load contribute to opening the O-ring seals and to large shell wall bending stresses at the vessel to flange transition regions. Undercutting mating surfaces ensures that the kinematics of the deformations will be as assumed and appears to be the best design procedure.

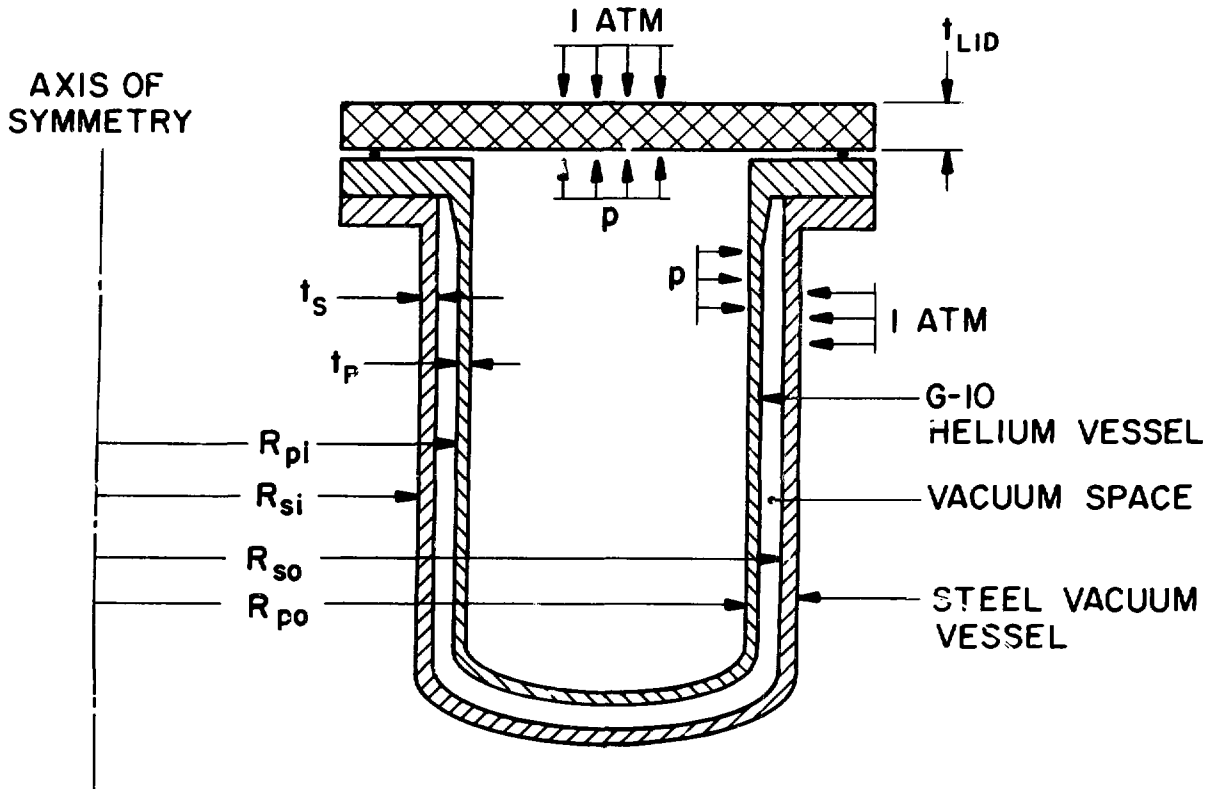


Fig. 4. Loading and nomenclature for dewar vessel and flange analysis.

Both noncomputer and finite element computer calculations were made. Figure 5 shows a typical finite element mesh used to study the lid and single flange combination. With this type of finite element mesh, the lid and flange displacements and rotations were examined for both normal operating load and fault condition loading to determine O-ring opening and the maximum flange to shell transition stresses. The length of the transition region and its thickness were also varied to study the effect on the shell bending stresses.

Both double flange and single flange designs appear feasible. The final design examined was the 2.5 in. thick by 7 in. wide flange with a small transition region representative of a fillet and a 1 in. vessel wall. Stresses during fault condition in both the flange and shell wall were less than 5 ksi. Stresses in the bolt region were about 15 ksi. O-ring opening displacements were around 0.005 in. and is an acceptable design. Because the model is axisymmetric, the bolt circle is a smeared region with material properties derived to keep the axial stiffness of the material correct for a ring of bolt material and G-10 plastic under an axial loading. Such representation does not allow a good evaluation of bolt stresses, and they should be analyzed further for proper sizing. In all models of the exterior flange, the assumption was made that there were 96, 1 in. bolts on the bolt circle with a preload of 20 ksi.

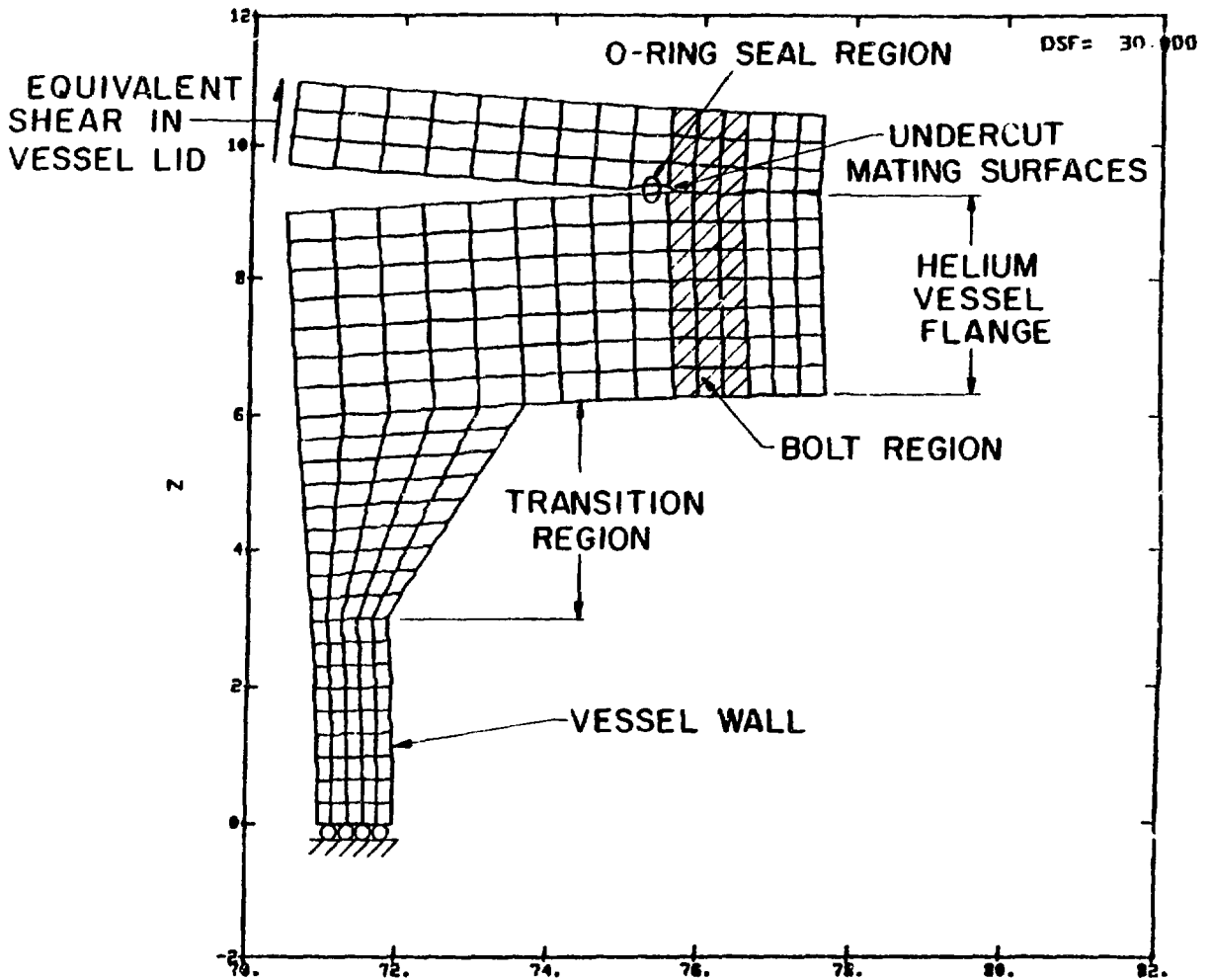


Fig. 5. Deformed finite element mesh of dewar lid to flange closure.

Two general comments can be made about the closure. The best designs are those that keep the bolt circles as close to the vessel walls as possible, and O-ring seals should be kept as close to the bolts as possible.

2. Cryogenic Design. A dewar vessel in the shape of an open mouthed container is standard in small sizes but highly unusual in the size needed for the 30 MJ coil. Because the vessel has a vertical surface area of roughly 50 m^2 and a room temperature lid with an area of 5.9 m^2 above the liquid helium, improper cryogenic design could produce excessive losses. Sources of heat leak considered are conduction from the top as the largest heat source, 324 W, and is composed of conduction through the helium gas, 191 W; through the vessel walls, 83 W; through the shear panels, 27 W; and through the

vertical struts, 23 W. Fortunately, these contributions may be reduced by allowing the helium gas generated to convect upward to form a counterflow heat exchanger. This system utilizes the large sensible heat of the gas rather than merely its small latent heat. As a penalty, the heat leak appears as a liquefaction load on the refrigerator rather than as a refrigeration load. The actual reduction in heat leak depends upon the detailed dependence of thermal conductivity versus temperature. Numerical calculations give a predicted heat leak of 9.9 W and a boiloff of 14.0 l/hr of liquid helium.

Radiation heating from the vessel walls and bottom will be reduced by the use of superinsulation, which will consist of approximately 100 layers of double aluminized Mylar alternating with Nylon* paper. Use of a liquid nitrogen shield was rejected as not being cost effective, largely due to its geometrical and structural complexity. The heat leak through the superinsulation cannot be calculated accurately because of uncertainty in the effective thermal conductivity. A conservative $k = 1 \times 10^{-6}$ W/cm-K value leads to a refrigeration load of 20 W. Radiation from the lid, 30 W, must be reduced by the use of multiple reflecting surfaces. The remaining heat load can be absorbed by heat exchange with the counterflow helium gas. Perhaps the most difficult problem will be to make radiation paths small around the many penetrations through the reflecting shields. A liquefaction load of 1 l/hr is assigned to this heat source.

Power leads represent a liquefaction load, when carrying current, of 1.5 l/kA-h/lead for a total load of 15.0 l/hr. When not carrying current, the load will be 8.0 l/hr.

The background heat load, before the coil is energized, would appear to be 23 l/h plus 20 W, but these are not additive. Detailed numerical calculations indicate when the gas boiled off by radiation, 28 l/h, is used to cool the power leads and conduction sources, that very little additional heat leak results from these sources. The total background heat load is thus expected to be 30 l/h.

E. Coil and Dewar Structural Support (Henke, Schermer; Bennett, Butler, Ferdinand, Q-13)

At Tacoma, WA the 30 MJ system will be installed in a Zone C seismic region, with design accelerations of 0.24 g horizontal and 0.16 g vertical, based on a 135 yr earthquake. Because support of a superconducting coil against seismic loads has never been addressed previously, there are no existing conceptual guidelines and a significant engineering effort was required. Other large magnets are usually supported against the walls of a metal dewar, which is constructed piece-by-piece about the coils and welded closed. This approach is not suitable for a plastic dewar, which should be constructed completely without seals or joints to be free of helium leaks. The design of a stiff support system is necessary to suspend the coil freely within a separately constructed, open mouth helium vessel.

*duPont trademark.

The method used to design the structure is an application of the seismic response spectra technique.^{2,3} Figure 6 shows the seismic response spectra for this site as supplied by BPA. This figure represents the maximum response that a single degree of freedom system, 1 mass and 1 spring, will have to an earthquake. To apply the technique, a linear structural model is formulated and a modal analysis is performed to determine the modes of vibration for the structural model. Because the modal analysis decouples or transforms the structural system equations of motion into a set of single degree of freedom equations, the maximum contribution of each mode to response of the structure in a site related earthquake can be determined using Fig. 6. The inverse transformation gives the maximum modal responses of the structure. These modal responses must be combined in some manner to determine the expected actual maximum response of the structure; and because no phasing information is available from Fig. 6, a statistical method is used. The combination rule used in this design is commonly referred to as the "square root of the sum of the squares" or SRSS method. Because closely spaced modes are more likely to add through phasing, a special rule of combination is followed for these modes. The procedures for combining modal responses used in the design are set forth in Ref. 4.

The seismic response spectra design technique can be applied to any structural model. The vehicle of implementation chosen for the 30 MJ SMES design was to program the method into the interactive finite element structural computer code called SPAR.⁵

With the combined finite element analysis and seismic response spectra technique, several designs for the support structure were investigated, each evolving from the results of the previous analysis.

The initial investigation assumed the coil to be a rigid body supported from the dewar lid by a pinned truss arrangement. The lid was reinforced at the support points with beams that spanned the width of the lid and rested on 12 supporting pillars. Figure 3 shows a cross section of the conceptual design and Fig. 7 illustrates the computer model and shows rigid links connecting the coil center of gravity to the supporting trusses, the dewar lid, and the upright supporting pillars. This initial design was acceptable in terms of the support structure itself, with relatively low stress levels and coil displacements. However, the horizontal force component from the truss supports to the coil attaching points indicate force levels equivalent to around 2 g's acceleration. The coil design relies upon frictional restraint against relative horizontal slippage between the coil top plate and the clamping beams which hold the pancake coil together. The clamping force was insufficient to provide the required frictional resistance during coil operation.

The next design investigated the same truss arrangement but also supported the coil against horizontal motion off the dewar wall. By taking advantage of a load path through the dewar wall, the acceleration levels in the coil were reduced to acceptable levels, but numerous problems arise with the details of such a design, particularly during assembly.

Study of the first two analyses revealed that an alternative design was possible. This design is the currently used scheme and partially decouples

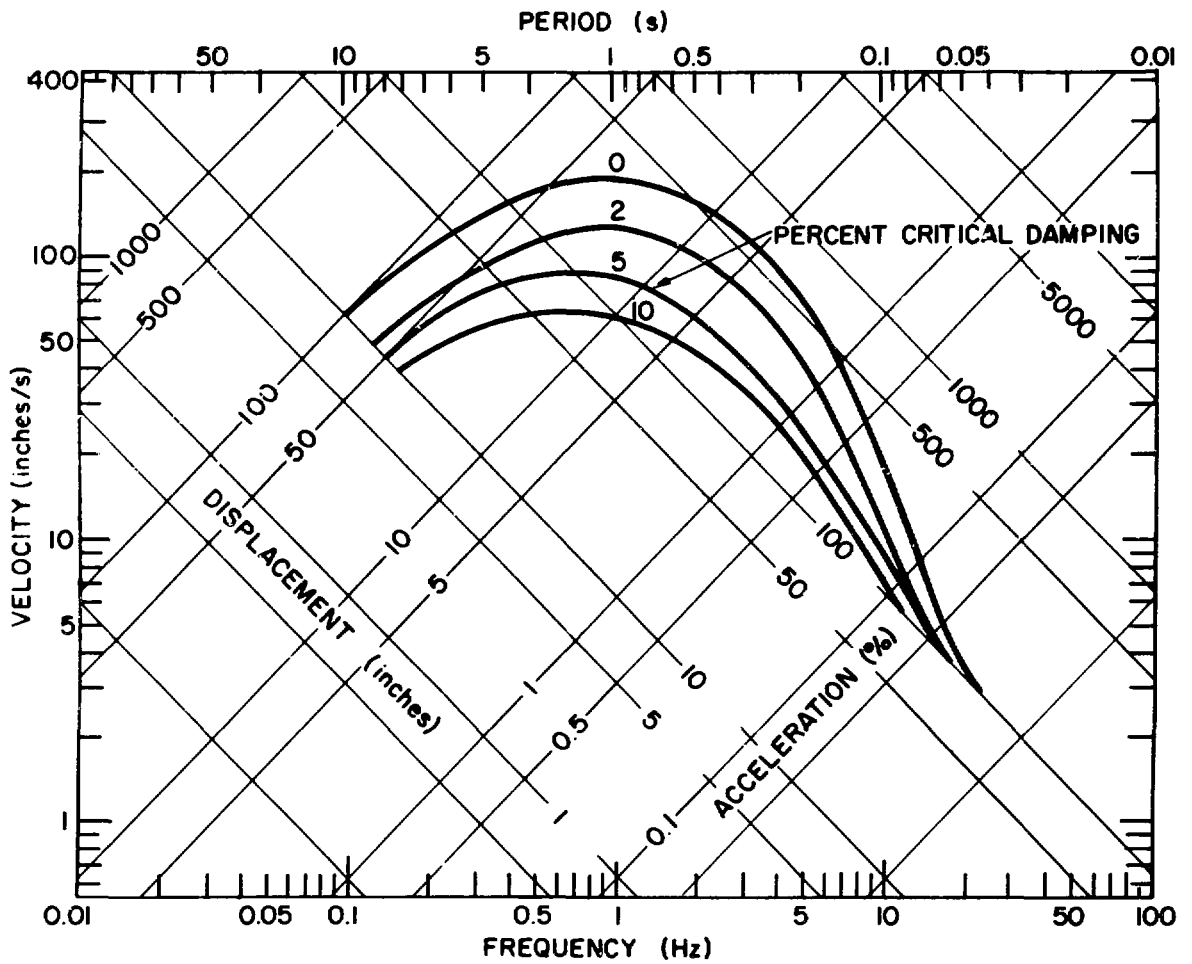


Fig. 6. Seismic design response spectra for the BPA site.

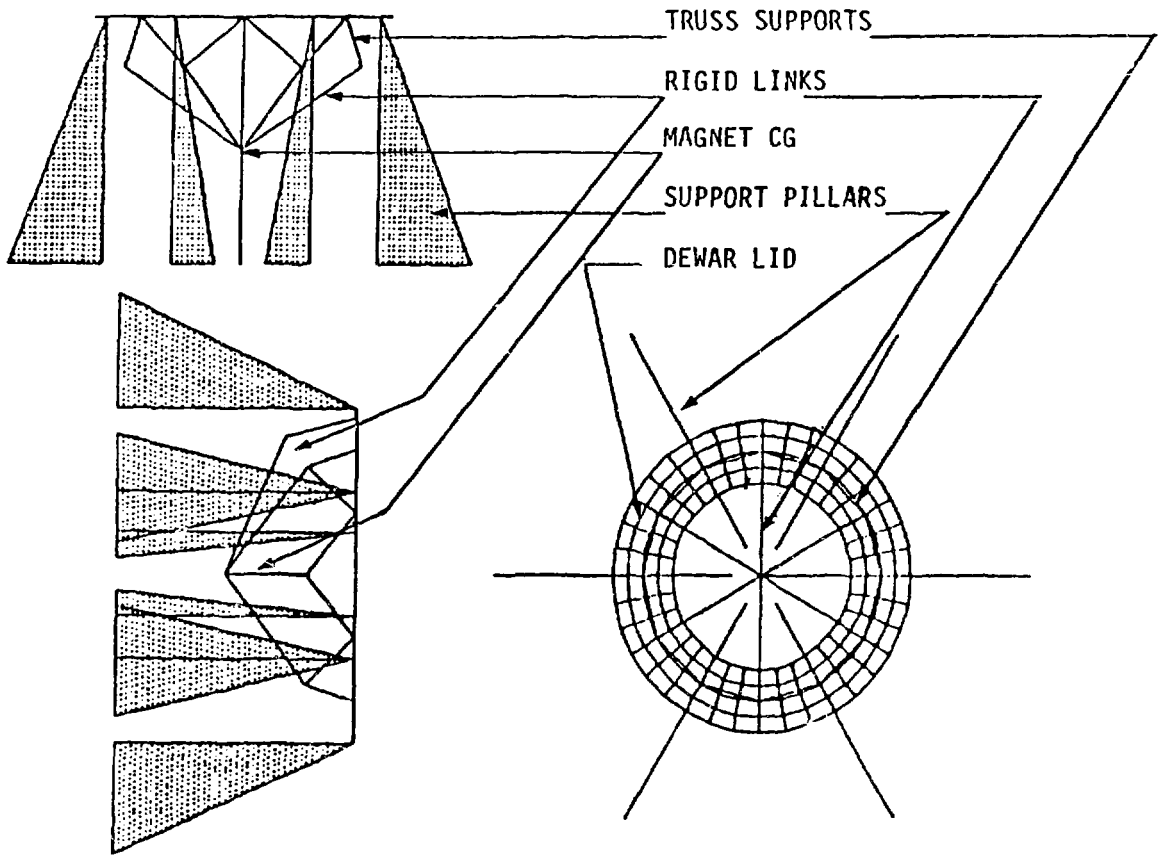


Fig. 7. Computer model of the initial structural support concept, not to scale.

the horizontal and vertical forces being input to the coil top plate. Conceptually, the design works in the following way. The large horizontal forces are resisted by vertical plates that effectively act as shear panels. Kinematic joints which resist only horizontal motion at the top of these panels prevent the large vertical force components associated with the coil swinging modes from unloading the coil clamping mechanism. The vertical motions and dead load are resisted by stainless steel tubes pinned at both ends in such a manner that only vertical motions are resisted by these members. Vertical and horizontal forces input to the coil top plate can be completely uncoupled by placing the kinematic joints at the shear panel to coil connection rather than at the shear panel to lid connection. However, the kinematic joint would be positioned in the liquid helium, which may require a development and testing program to ensure successful operation. In the final design, the joints are at the top of the panels. This somewhat couples the vertical and horizontal motion, but the vertical forces from the lateral and vertical vibration modes interface with the coil at different locations. This separation is enough to prevent unloading of the pancake coil clamping mechanism. The current configurations and dimensions of the support system design are illustrated in Figs. 8 and 9.

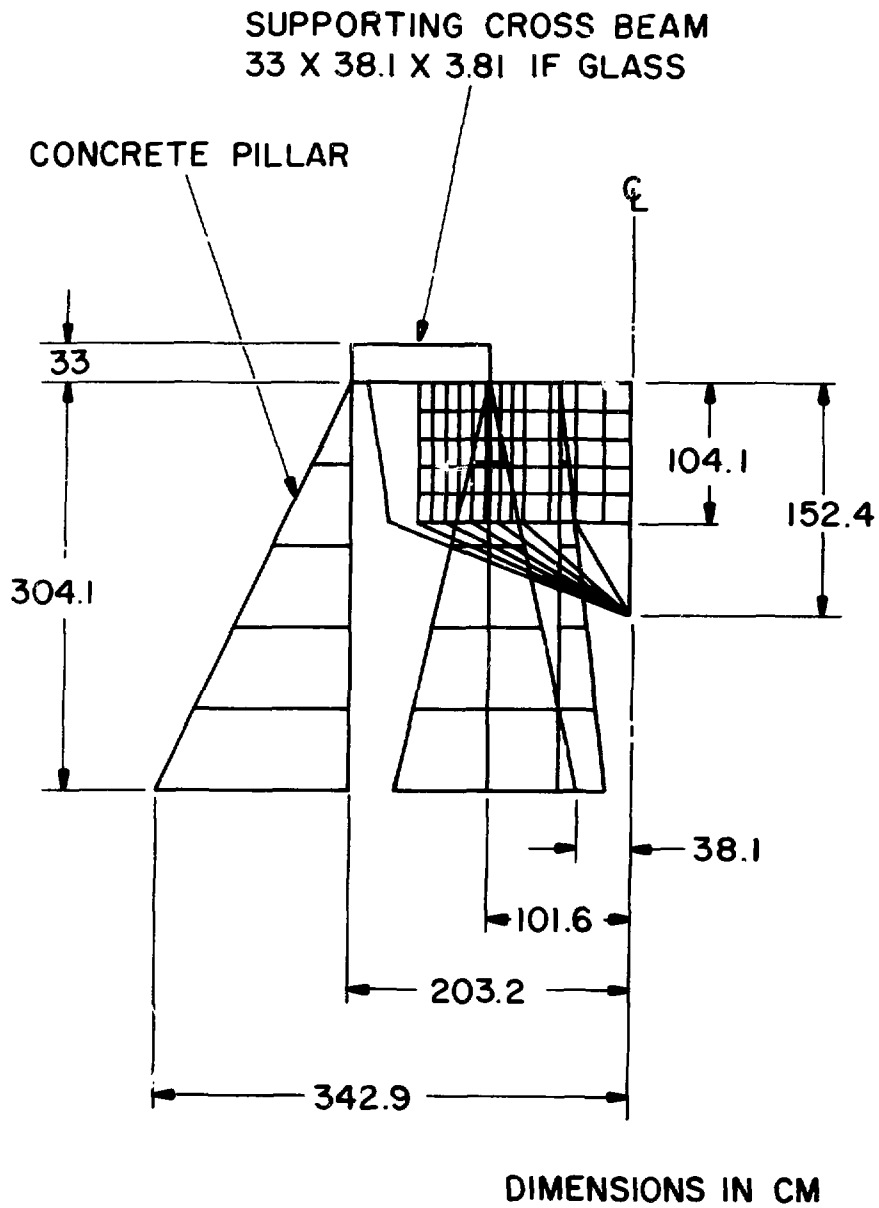


Fig. 8. Current design of the structural support concept with dimensions.

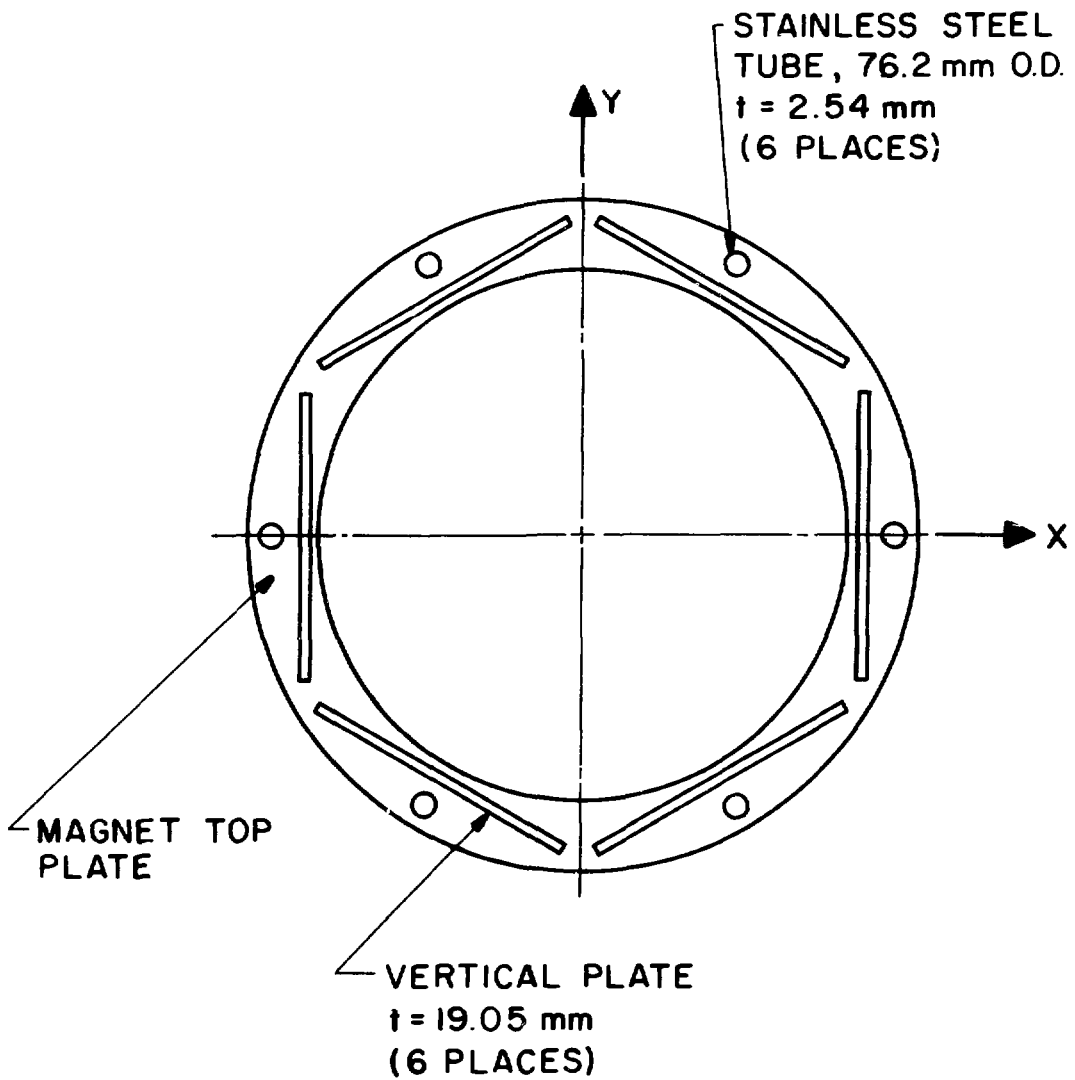


Fig. 9. Plan view of current design of the support concept illustrating shear panel and vertical strut placement.

In all designs considered, a much better coil design results if the individual pancake coils are pinned against lateral shear. Thus, during assembly the coils are pinned together.

During the evolution of this design several variations were examined. One of the most notable was a concept that reduced the maximum response of the coil by using shear panels with different shear thicknesses. In effect, this design ensured that the frequencies of the two fundamental modes, that is, the lateral modes in the two orthogonal directions, were not closely spaced. This concept proved very effective when vertical and lateral motion were completely decoupled. However, when the kinematic joints were moved to the top of the panels, these frequencies could not be adjusted so easily. In the final sizing and geometry of the support structure, an adequate and more convenient design resulted with all panels being the same thickness.

The effectiveness of the design requires that the structural stiffnesses of the final model must be maintained during the detailed design to ensure the maximum response will be as predicted. Investigation of other geometries may produce an equivalent design, but may prove more costly in manpower and computational time than material or space savings can justify.

F. Helium Vapor Cooled 5 kA Electrical Leads (Henke, Schermer)

Each second subcable must have its own power lead to provide a series resistor to balance the current in the 5 kA cable. The 10 leads are to be made into a single mechanical package for convenience of manufacture and insulating. The conceptual design utilizes 10 parallel copper plates about 0.3 cm x 3.0 cm in cross section, supported within a rectangular G-10 box, with the plates electrically insulated from each other except at the room temperature end, where they join the busbar to the converter. Counterflow helium gas is brought up 1 mm gaps between the plates to provide cooling. The plates are grooved vertically to provide extended cooling surface. Horizontal fins would be preferred because they add surface and mass without adding to the thermal conduction down the lead; however, such fins could cause electrical shorting and channel blockage if neighboring plates experience differential thermal contraction. Possible thermohydraulic instabilities in parallel flow channels are eliminated by ensuring that the exit gas from each channel warms to room temperature and establishing the pressure drop in each channel by passing the warm gas through orifices. All thermal and mechanical computations have been made for the lead and a layout drawing has been prepared.

Additional thermal stability is obtained by using copper plates with a low RRR. Suitable copper alloys normally are fabricated as tube rather than plate. Plate is available if 1000 to 2000 lbs is ordered, although the leads require less than 100 lbs. Alternate sources are being sought.

G. Cryogenic System (Dean, Harkleroad, Henke, Holguin)

A complete cryogenic system is being manufactured and assembled to provide the liquid helium and gas storage for the 30 MJ coil. Plans and designs for separate trailers were made for testing the entire cryogenic system at Los Alamos and subsequent transport to Tacoma, WA. The SMES system will be operated by automatic controls through a computer with control inputs from Portland, OR.

1. Refrigerator. CTI - Cryogenics mounted a 90 l/h helium refrigerator/liquefier in a Los Alamos supplied trailer. The trailer mounted unit failed an acceptance test at the manufacturer's plant on 1/28/80. A number of recommendations were made that CTI incorporated into the system and another acceptance test was performed. The required liquefaction rate was met, but one of the compressors overheated. The coolant plumbing to the compressors was replaced with larger pipes and the system was shipped to Los Alamos in September 1980.

A piping pressure check showed that a leak existed between the cold box piping and the insulating vacuum. A broken 1 in. pipe was found at a turbine outlet. CTI sent a welder and engineer to Los Alamos to repair this pipe. Further checking revealed other leaks in locations that were inaccessible. The refrigeration trailer was returned to CTI for repair.

The damage was caused by inadequate support of the cold box heat exchangers and plumbing in the vacuum tank during shipment. One support bolt had bent causing the heat exchangers and plumbing to sway freely during shipment. CTI will improve the support system for shipping.

The SMES system dewar and coil will not be operated at Los Alamos. A heat load is being constructed to test the helium refrigeration system. The load consists of a 4 ft diam dewar fitted with temperature sensors, level sensors, and heaters. Power input to the heaters will be stepped and ramped to determine the response of the refrigeration controls. The heat load assembly is near completion.

2. Heat Rejection System. A heat rejection system, consisting of a cooling tower, coolant tank, valves, coolant circulating pump, and controls, mounted on a trailer, was assembled by a mechanical contractor and delivered to Los Alamos. This system will be used to absorb 300 kW of heat from the refrigeration system compressors and the gas recovery system compressors. The mechanical contractor did not have the capability of testing the heat rejection system under full load. This system will also be used to cool the 1.25 MW resistive load for testing the converter. This operation will provide an opportunity to check the heat rejection system controls.

The heat rejection unit is located in the left foreground of Fig. 10. The white CTI refrigerator trailer is in the center rear of the picture, and the damaged cold box heat exchanger is on a stand for inspection to the right far rear of the picture.

3. Gas Recovery System. When the SMES unit is warmed, a large volume of helium gas will evolve. A recovery system is being constructed by a mechanical contractor. The system consists of surge tanks, compressors, and controls. This trailer mounted system will deliver gas at a pressure of up to 2400 psi to a railroad tank car on a siding at the Tacoma Substation. Diaphragm compressors are used that are dynamically unbalanced. An attempt was made to isolate the dynamic load from the trailer by using spring mounts and damping shock absorbers. Only partial force isolation was achieved, and the large compressor amplitude was judged to be undesirable. The compressors will be mounted rigidly to the trailer floor and the floor reinforced to withstand the dynamic load.



Fig. 10. Heat rejection unit, refrigerator trailer, and cold box heat exchangers.

H. Electrical System

1. Converter. (Boenig, Smith, Trudell, Turner) The ± 2.5 kV, 5 kA, 12 pulse, air cooled converter was designed and built by Robicon Corporation. The unit was shipped to Los Alamos after extensive acceptance tests. During the tests the converter was loaded with 110% of rated current at low voltage for three hours and was operated at 110% of rated voltage at low current level. The control logic of the two converter bridges, the two bypasses, the dc breaker, and the fan unit was checked by simulating anticipated faults, such as line loss, line overvoltage, line unbalance, overcurrent, thyristor heat sink overtemperature, ground fault, loss of air flow, loss of thyristor fuse, etc.

The total converter system including the energy dump circuit will be tested at Los Alamos at full current and ± 250 V dc in the automatic control mode. An existing 3.25 MVA six phase transformer system is available for 12 pulse converter operation.

The converter power cabinet and the fan unit, shown in Fig. 11, were positioned at the SM-32 site. The converter control cabinet was mounted in the control and instrumentation trailer. This trailer is located 200 ft from the converter power cabinet, which measures 9.5 ft wide by 10.9 ft high by 18 ft long. Multi-cable connections for 13 analog signals, 75 digital signals, and the control and auxiliary power were installed between the control trailer and the converter cabinet. The converter control and instrumentation



Fig. 11. 10 MW converter power cabinet with forced air cooling fan.

system was made functional and tested in the manual mode. Minor equipment failures caused by mechanical vibration during the transport and electrical noise interference between control signals and power lines were identified and corrected. An existing 25 kVA, six phase transformer and the timing transformers were connected to the converter bridges to make the converter functional for low voltage, low current operation and to check the firing logic. The converter bridges and bypasses function properly. The dc breaker control for the energy dump circuit will be tested first at low current levels. To check the converter system at 5 kA, a stainless steel, water cooled resistive load dump was designed and is being built.

The converter was dropped when being unloaded at Los Alamos. All physical damage has been repaired. Preliminary checks indicate no damage occurred to the electrical system. Further evaluation for damage will be determined during the high current testing.

2. 3.25 MW Rectifier ac/dc Power System. (Boenig, Buteau, Harkle-road, Loya, Turner) The ac power components of the 3.25 MW rectifier system will be used to supply six phase power to the SMES converter. During the initial checkout of the rectifier, an internal breakdown of the insulation in the 1.35 MVA induction voltage regulator (IVR) resulted in a line to ground fault that necessitated repair. The IVR was repaired, reinstalled, and successfully tested with a water cooled resistive load at 7 kA.

3. Transformers. (Boenig, Turner) Both 2 MVA power transformers were successfully tested at the Niagara Transformer Company plant and accepted by

Los Alamos. During the transport from Buffalo, NY to Tacoma, WA. one transformer fell from the truck and was severely damaged. This accident was caused by a malfunctioning of the air suspension system of the truck. The damaged transformer was returned to the manufacturer for repair. The second transformer and a 0.5 MVA General Electric service transformer were received at the Tacoma, WA Substation. The GE transformer was checked by BPA, found to have contaminated oil, and is to be returned to GE for corrective action. The 75 kVA GE transformer is being used at Los Alamos in the electric power system for the SMES system tests.

4. Transient Voltage Analysis. (Chowdhuri) Transient voltages in the 30 MJ SMES system might arise from effects such as operation of the superconducting coil protective energy dump circuit. Such effects were analyzed to determine if voltage and insulation ratings will be exceeded.

The response characteristics of the 30 MJ coil were determined both with a metal and nonconducting dewar. For transient analysis, a coil cannot be simply represented by its self and mutual inductances. The capacitances between turns and between coil sections as well as the capacitances between various parts of the coil to ground must be included. When a step function voltage is applied across a coil, it is initially represented as a capacitive network, and the inductances represent infinite impedances.

The initial voltage distribution along the length of a uniformly wound single layer coil can be determined by applying the standing wave theory. This initial voltage distribution is nonuniform, being higher at the line end or high voltage terminal of the coil in contrast to the grounded terminal. The nonuniformity of the initial voltage distribution is augmented by the capacitances of the coil elements to ground. The transition from the initial nonuniform voltage distribution to the final uniform distribution takes place through intermediate voltage oscillations.

In most cases, the voltage stress across the insulation between turns at the line end is of more concern than the voltage stress across the major insulation between a coil element and ground. The gradient of the initial voltage distribution at the line end is the voltage gradient across turns. The solution with the step function applied voltage can be used to determine the various voltages for any other type of applied voltage by Duhamel's theorem, provided the same capacitive network is used.

The simple standing wave theory cannot be applied when the winding structure is complex, such as for the double pancake coils of the 30 MJ SMES coil. For that coil, the problem was solved in two steps. First, the major voltage distribution from each coil to ground was determined from the total ground and series capacitances of the winding. The voltage across the first coil at the line end was determined. Second, from the voltage across the first coil, the voltage across the line end turns was determined from the turn to turn and pancake coil to pancake coil capacitances.

The analysis was performed for two cases, for the coil in metal and insulated dewars. The coil voltage distributions are shown in Figs. 12 and 13. Figure 12 represents the coil with one end solidly grounded, and Fig. 13 represents the coil with a high resistive impedance to ground. The curves through the circles and triangles are the initial condition peak amplitudes

when the coil inductance is effectively infinite and only capacitive characteristics are dominant. The curves labeled "envelope" represent the maximum initial condition voltage and is obtained by adding the difference between the steady state, infinite time voltages, given by the broken line, and the initial condition peak amplitude voltages to the steady state voltages. The voltages across the first two turns and first two pancake coils at the high voltage line end are shown in Table II. With an insulated dewar, the initial transient voltage distribution in the 30 MJ coil deviates very little from the steady state voltage distribution, and turn to turn transient stress will not be high.

Figure 14 shows the protective dump circuit of the 30 MJ SMES system at the output of the converters. The transient voltage of the vacuum circuit breaker, when it interrupts the SMES coil current, was analyzed.

The converter voltage is brought to zero and the two series strings of thyristors are fired before the vacuum breaker is opened. The precharged capacitor, C, is discharged through the arcing contacts of the vacuum breaker by firing the thyristor in the capacitor circuit. When the counterpulse current becomes equal to the arc current, the arc quenches and the coil current is diverted through C and R. The resistance, R, is installed to discharge the stored energy in the coil. L_2 is the self inductance of the resistor R.

Two components of voltages are impressed across the coil because of the current interruption. The first component is of positive polarity and is caused by the residual voltage in the capacitor, C, after arc interruption. The second component is of negative polarity and is caused by the negative rate of change of the interrupter current. The counterpulse current of equal magnitude and opposite direction to the interrupted current was simulated in the analysis by applying a phase shifted sinusoidal current across the opening contacts of the vacuum breaker. L_1 serves as a waveshaping counterpulse current inductor. The voltage drop across AB in Fig. 3 was calculated. The analysis was made with the assumption that current flows in both directions across the counterpulse thyristor. This will be the case if rectifiers are placed across the thyristor in antiparallel direction. Otherwise, the

TABLE II

VOLTAGES IN 30 MJ SMES COIL WITH 10 kV APPLIED STEP FUNCTION VOLTAGE

	<u>Metal Dewar</u>	<u>Insulated Dewar</u>
Voltage across first two turns, V	387	134
Voltage across first two pancake coils, V	1633	585

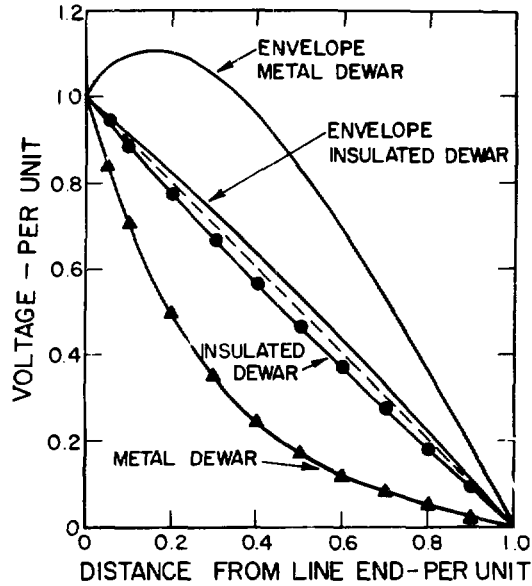


Fig. 12. Coil voltage as distance from line end or high voltage terminal of the 30 MJ SMES coil to ground when one terminal is grounded. The broken line represents infinite time, final voltage distribution.

capacitor branch will be shut off when current through the thyristor is below its holding current level. This will happen at about the time the negative peak of the voltage occurs, and the subsequent voltage oscillations will not occur.

Figure 15 shows the transient voltages across the coil for three sets of assumed system parameters. Curve 1 represents the anticipated transient voltage for $R = 0.9 \Omega$ and $L_2 = 600 \mu\text{H}$. Curve 2 represents the case with the same resistor and $L_2 = 20 \mu\text{H}$. The system stress is quite low under this condition. Curve 3 represents the case where $R = 0.45 \Omega$ and $L_2 = 300 \mu\text{H}$.

All three curves show a zero time positive peak. In practice, high frequency oscillations will be present because of the finite but small capacitance of the vacuum breaker in the open position. With a breaker capacitance of 15 pF and the saturated inductance of saturable reactor of 1 H , the frequency of these oscillations will be 10.4 MHz .

Since the analysis shown in Fig. 15, the self inductance of the protective dump resistor has been measured to be $35 \mu\text{H}$ and $100 \mu\text{H}$ by two different methods. Further measurements will be made. In any event, for $L_2 \leq 100 \mu\text{H}$, the transient voltage will not exceed the system rating for a counterpulse capacitor charged to 5 kV at full coil current of 4.9 kA .

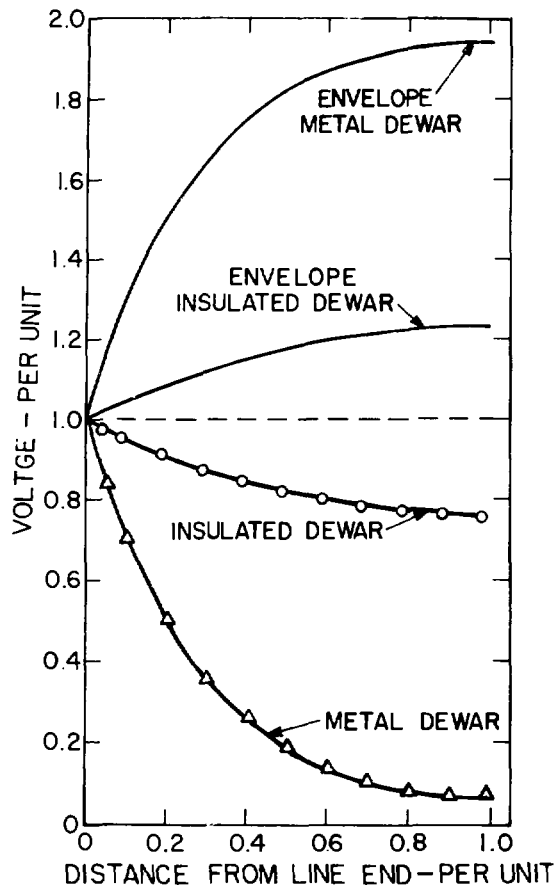


Fig. 13. Coil voltage as distance from line end or high voltage terminal of the 30 MJ SMES coil to ground when one terminal is tied to ground with high resistance. The broken line represents infinite time, final voltage distribution.

Transient voltages from external sources were not considered for this analysis. Although surge protectors are applied at several places on the ac side of the converters, these may not be adequate for the protection of the coil system. To an external transient, the SMES coil may look like a coil grounded through high impedance, depending upon the size and type of the grounding resistor. An obvious improvement will be to connect a $1 \mu\text{F}$ capacitor and a low voltage, high energy varistor across the grounding resistor to reduce the transient grounding impedance. A low resistance station grounding grid must be available.

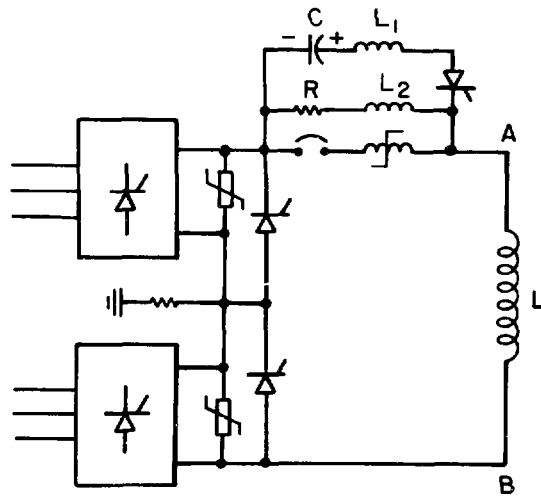


Fig. 14. Protective dump circuit of the 30 MJ SMES system.

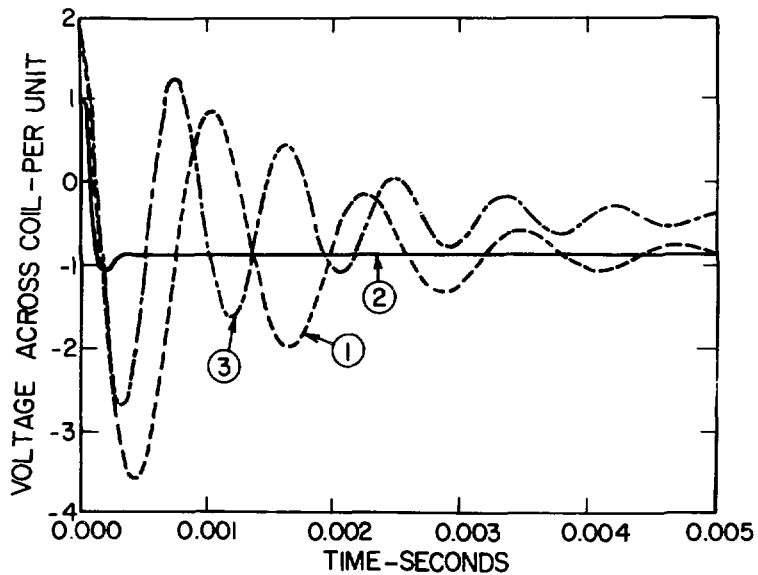


Fig. 15. Transient voltage across 30 MJ coil caused by vacuum breaker opening. Curve 1 : $V_C = 5$ kV, $I = 4.9$ kA, $L_1 = 15$ μ H, $L_2 = 600$ μ H; Curve 2 : Same as Curve 1, except $L_2 = 20$ μ H; Curve 3 : Same as Curve 1, except $L_2 = 300$ μ H, $R = 0.45$ Ω . The per unit voltage = counterpulse capacitor charging voltage.

I. Control and Data Acquisition System (Boenig, Smith, Trudell, Turner; Conley, E-5; Criscuolo, E-8)

The control and data acquisition (CDA) subsystem will function as the central communications point of the SMES system. The CDA system will respond to commands from BPA, or a local operator, by adjusting SMES system control parameters and will determine the system's state by monitoring data from each of the subsystems.

The tasks required of the CDA system will be divided among three LSI 11-23 computers from Digital Equipment Corp. The organization of the CDA system is illustrated in the CDA system block diagram, Fig. 16.

The controller will function as the central communications point and supervisor for the CDA system. It will accept information from BPA or the local operator, which describes the desired state for the SMES system. The current state of SMES is described by the information from the cryogenic data acquisition system (CDAS) and the energy data acquisition system (EDAS). After comparing the information from these sources, the controller adjusts the control parameters to bring SMES to the new state being requested. The controller will also display the state information to the operator and BPA.

The state of the SMES system will be monitored continually by the CDAS and EDAS. These subsystems are capable of acquiring data at a high rate and storing the data for post failure examination. Attaining a high data rate is the primary reason for separating the control function from the monitoring function. The CDAS and EDAS will be responsible for reporting parameter limit excursions to the controller.

The CDA system will provide the following capabilities to the SMES system.

- a. Unmanned control of the system for extended periods of time as long as weeks to months.
- b. Data storage that will aid in analyzing system performance and diagnosing system faults.
- c. Display system performance in a manner that facilitates system operation and maintenance.
- d. Safe and reliable shutdown of the system during emergency conditions.

Significant progress was made in procuring the components of the CDA system, defining the signal interface between the CDA system and each of the other subsystems, constructing the control room in the Control and Instrumentation Trailer (CIT), initiating the design of an instrumentation amplifier for signals originating at the dewar/coil, and initiating the design of the control software.

All of the major components for the controller, EDAS, and CDAS were received. These include computer chassis, central processors, memory, inter-processor serial communications boards, parallel input output boards, analog

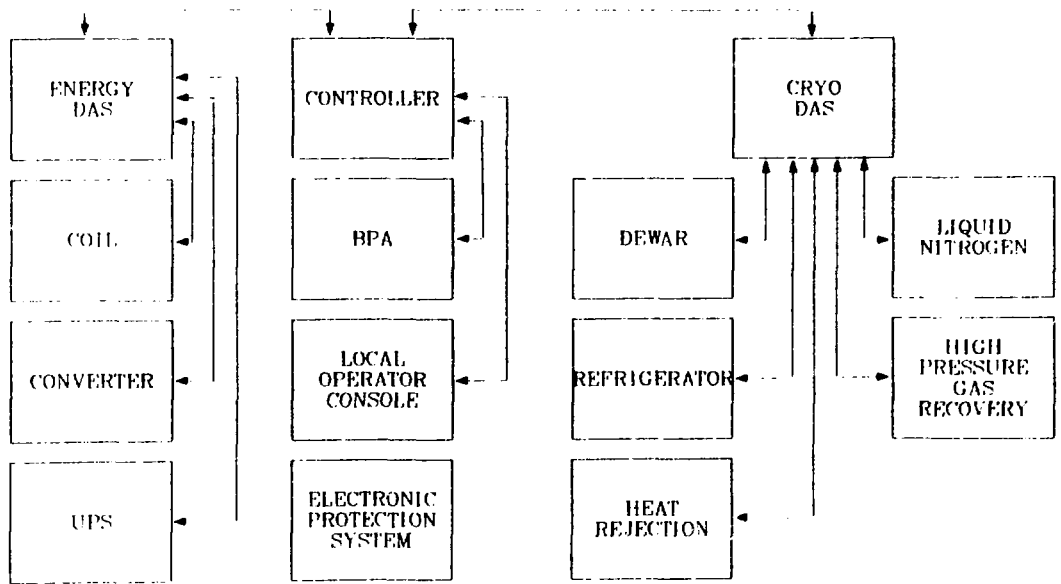


Fig. 16. Control and data acquisition system block diagram.

to digital converters, timers, stepper motor controllers, console, printer, mass storage device, and electronic enclosures. These components are presently going through initial checking and integration.

The signal interface between the CDA system and each of the other subsystems, with the exception of the dewar/coil and electronic protection, was defined. All of the cables required to complete these signal paths to the CIT were designed and fabricated. All of the signal paths terminate at a single junction box in the CIT. The assembly and wiring of this junction box is completed. Checking and integration of the junction box with the CDA system is expected to be done early next year.

As part of the signal interface definition task, the clean ac power distribution and grounding were designed. Three ultra high isolation transformers were purchased and installed. An evaluation of uninterruptible power supplies was completed, and a request for quotation was initiated.

Construction of the control room in the CIT is well under way. Installation of the instrumentation power, cable gutters, air conditioning, electronic enclosures, junction box, converter control panel, and flooring is completed. The clean ac power was checked and many of the instruments have been powered.

A design of an instrumentation amplifier for dewar/coil diagnostic signals was initiated. The schematic is completed and a breadboard was statically tested. Dynamic and environmental testing will begin early next year.

The control logic is in an advanced state of development, and preliminary design of the control software for the refrigerator and gas recovery subsystems was completed. Completion of the preliminary design software for the other subsystems is expected early next year.

J. BPA Site Installation (Boenig, Henke, Rogers, Schermer, Turner)

BPA engineering representatives visited Los Alamos to discuss the SMES installation at the Tacoma Substation and to develop proposed task assignments on the electrical, mechanical, and cryogenic systems. Site layout details were determined and a site plan drawing was made. Operational safety and guidelines for working relations with crafts were defined. The Interface Working Agreement for the Development, Installation, and Testing of a Superconducting Magnetic Energy Storage (SMES) System at BPA's Tacoma Substation among DOE, BPA, ALO Office, and LASL, now the Los Alamos National Laboratory, was put in place with all parties signing.

K. SMES Test Area at Los Alamos (Boenig, Henke, Schermer, Turner)

The SMES systems layout for operation and testing at Los Alamos was designed to duplicate the operation at the Tacoma Substation. Plumbing between trailers, which can also be used in the BPA installation, was specified and fabricated. Electric power, required for the helium refrigerator, heat rejection unit, and gas recovery unit, was installed; electrical protection devices were installed; and control cables, which will also be used at BPA, were made.

III. 1 TO 10 GWh SMES DIURNAL STORAGE UNIT (Costello, Consultant)

In the previous year a reference design was completed for a 1 to 10 GWh SMES diurnal load leveling system. As a part of that study, a simple superconducting cable concept, based upon a supporting wire rope cable, was put forward. Such a superconducting cable would cost less, would be easier to fabricate in situ, if required, and lends itself more readily to joining than conductors previously proposed. A consultant, an expert in wire rope technology, was hired to evaluate the structural aspects of the concept. The evaluation clearly showed that the concept is promising. One example analyzed showed that a 304 stainless steel wire rope with 4921 strands of 0.017 in. diam, supported on 2 m centers with a total cross sectional area of 1.15 in.² can readily support the necessary superconducting strands wrapped in helical array on the outside. The example chosen is for a 50 kA cable in a 4.5 T field. The design of the example is well within the state of the art for wire rope.

IV. SUPERCONDUCTOR APPLICATION VAR (SAVAR) CONTROL

A. Introduction

Thyristor phase controlled reactors with a parallel connected capacitor bank are now used in static VAR systems to compensate for lagging load currents and to eliminate unbalanced loading of three phase power systems. In principle, a static shunt compensator consists of three air core reactors

arranged in a delta configuration and connected to a pair of antiparallel thyristors. A three phase capacitor bank provides a constant leading power factor. Reactor currents can be varied continuously from zero to the maximum value by proper phase control of the thyristor switches, thereby controlling the lagging power factor. Compensators with a power rating of 20 to 100 MVAR connected to a 13.8 or 34.5 kV bus typically have 1.2% losses. These losses can be broken down into 0.15% capacitor losses, 0.6% reactor losses, and 0.45% SCR losses.

Low frequency dc superconducting coils have low losses and can be used in a VAR circuit as a replacement for a conventional inductor. A direct replacement of the room temperature coils by conventional superconducting coils would not result in a system with lower losses. The current in the coil is essentially constant but some 360 Hz harmonic exists in the coil and in the line currents. The superconducting coil must have acceptably low losses at this frequency.

B. Experimental Results (Boenig, Rogers, Smith, Singleton, Trudell)

A six pulse SAVAR prototype unit was tested with a 14 H, 5 Ω room temperature and a 7 H superconducting coil as inductors. The tests verified the theoretical predictions. Tests were performed with both delta-delta and delta-wye transformer connections. The recorded wave shapes for the line currents and voltages and the reactive power show very good agreement with those predicted. In the experiment, the reactive power was varied continuously in the range of 20% to 100% of the rated power. In addition to different six pulse experiments, a hybrid 12 pulse SAVAR circuit was tested. One secondary winding of a six phase power transformer was connected to an uncontrolled diode bridge with the other winding connected to the SCR bridge. The experimental results show good agreement with the theoretical curves. The line current harmonics were verified for different reactive power values.

C. Application Possibility (Boenig)

The application possibility of a SAVAR circuit was extended conceptually to use in exciter systems of superconducting generators and in series connected, line commutated converters for reactive power minimization.

D. Contracts for SAVAR Optimization (Boenig, Rogers)

Two contracts to make SAVAR coil and converter comparison optimization studies were placed with Westinghouse Electric Co. The technical findings are as follows. Several superconducting coil concepts, as components integrated into VAR control systems of 40, 50, and 100 MVAR, were examined by means of a parametric study. Only at 100 MVAR did appreciable savings appear. Still, at 100 MVAR these were limited to a 7.5% and 15.5% cost saving spread over 30 years of operation without any cost of money included. Energy losses were costed at \$2000/kW. Even at \$3000/kW for loss cost, the savings only increased about 5%. These values are too low to demonstrate economic advantage at this stage of concept. The types of superconducting coil systems studied included shielded, nonshielded, air core, iron core, dc, and ac.

All the systems required very expensive high technology, but the systems were costed at values close to production state of the art technology as if a market for 100 units existed.

The high technology requirements called for

- a. 0.5 to 1.0 m superconductor filaments,
- b. Nb₃Sn superconductor,
- c. 0.003 to 0.005 in. diam superconducting strands,
- d. Nonconducting dewar,
- e. 40 kV withstand voltage,
- f. Noncryostable braided cable,
- g. Elaborate electrostatic shield integral with the coil winding, and
- h. For the air core, shielded, ac coil system with the most favorable cost saving, a difficult superconducting switching operation of current between the shield coil and the main noncryostable coil is required for fault mode operation.

V. MISCELLANEOUS

A. 20 kJ SMES Demonstation Unit (Boenig, Turner)

The 20 kJ SMES energy storage unit was operated at the Energy Technology Conference, Washington, DC and the Los Alamos open house, Family Days. The demonstration unit stores energy in a superconducting coil. This stored energy was subsequently used to power an incandescent light and to drive a cassette recorder for playing music. The demonstration unit was incorporated in the Los Alamos award winning exhibit at the New Mexico State Fair.

VI. PAPERS PRESENTED AND REPORTS

1. P. Chowdhuri, "Behavior of Thyristors under Transient Voltages," IEEE PES Winter Meeting in New York, February 3-8, 1980, Paper No. A80 114-9; IEEE Publication No. 80CH1523-0-PWR, 1980.
2. P. Chowdhuri and M. A. Mahaffy, "Wave Propagation in a dc Superconducting Cable Part I: Analysis," Paper No. 80 SM 617-1, and "Wave Propagation in a dc Superconducting Cable Part II: Parametric Effects," Paper No. 80 SM 618-9; Summer Meeting, Minneapolis, MN, July 13-18, 1980.
3. P. Chowdhuri, "Some Characteristics of Dielectric Materials at Cryogenic Temperatures for HVDC Systems," IEEE Trans. Elec. Insulation, Los Alamos Scientific Laboratory report LA-UR-80-1568.

4. John D. Rogers, "Magnetic Energy Storage," Applied Superconductivity Conference, 1980, September 29-October 2, 1980, Santa Fe, NM.
5. R. I. Schermer, H. J. Boenig, M. Henke, and R. D. Turner, "Conductor Qualification Tests for the 30-MJ Bonneville Power Administration SMES Coil," Applied Superconductivity Conference, 1980, September 29-October 2, 1980, Santa Fe, NM.
6. H. J. Boenig, LASL and W. V. Hassenzahl, LBL, "Application of Superconducting Coils to Reactive Power Control in Electric Power Systems," Applied Superconductivity Conference, 1980, September 29-October 2, 1980, Santa Fe, NM.
7. E. Hoffman, J. Alcorn, W. Chen, Y-H Hsu, J. Purcell, General Atomic Company and R. Schermer, LASL, "Design of the BPA Superconducting 30-MJ Energy Storage Coil," Applied Superconductivity Conference, 1980, September 29-October 2, 1980, Santa Fe, NM.
8. W. M. Parsons, LASL and R. J. Wood, ORNL, "Protection Circuits for Superconducting Magnets," Submitted to Fourth ANS Topical Meeting on Technology of Controlled Nuclear Fusion, King of Prussia, PA, Oct. 14-17, 1980.
9. G. Costello, (Consultant for LASL), University of Illinois at Urbana-Champaign, "Wire Rope Superconducting Cable for Diurnal Load Leveling SMES," Mechanical, Magnetic, and Underground Energy Storage 1980 Annual Contractors' Review, Washington, DC, November 10-13, 1980.
10. R. Schermer, "30-MJ Superconducting Magnetic Energy Storage for BPA Transmission Line Stabilizer," Mechanical, Magnetic, and Underground Energy Storage 1980 Annual Contractors' Review, Washington, DC, November 10-13, 1980.
11. Richard T. Byerly, Westinghouse Electric Company and Jose A. Juves, Westinghouse Electric Company, "Effects of SMES Units on Power System Stability," Mechanical, Magnetic, and Underground Energy Storage 1980 Annual Contractors' Review, Washington, DC, November 10-13, 1980.
12. John R. Purcell, General Atomic Company, "30-MJ Superconducting Coil Design and Fabrication," Mechanical, Magnetic, and Underground Energy Storage 1980 Annual Contractors' Review, Washington, DC, November 10-13, 1980.

REFERENCES

1. ASME Boiler and Pressure Vessel Code, 1977 edition.
2. R. W. Clough, "Earthquake Analysis by Response Spectra Superposition," Bull. of the Seismological Soc. of Am., Vol. 52, No. 3, pp 647-660, July 1962.

3. R. W. Clough and J. Penzien, Dynamics of Structures, McGraw Hill (1975), New York.
4. "Design Response Spectra for Seismic Design of Nuclear Power Plants," US Nuclear Regulatory Guide 1.60, Oct. 1973.
5. W. D. Whetstone, "SPAR Structural Analysis System Reference Manual," NASA report NASA-CR-145098-1, Vol. I (February 1977).